

**Effect of ether glycerol lipids on interleukin-1 $\beta$  release and experimental autoimmune encephalomyelitis**

Stephanie D. Boomkamp<sup>a</sup>, Hoe-Sup Byun<sup>b</sup>, Satvir Ubhi<sup>a</sup>, Hui-Rong Jiang<sup>a</sup>, Susan Pyne<sup>a</sup>,  
Robert Bittman<sup>b</sup>, Nigel J. Pyne<sup>a</sup>

<sup>a</sup>Strathclyde Institute of Pharmacy and Biomedical Science, University of Strathclyde,  
Glasgow G4 0RE, UK; <sup>b</sup>Department of Chemistry and Biochemistry, Queens College, The  
City University of New York, Flushing, NY 11367-1597, USA

Correspondence to NJP (mailing address: Strathclyde Institute of Pharmacy and Biomedical  
Science, University of Strathclyde, Glasgow G4 0RE, UK. e.mail:n.j.pyne@strath.ac.uk; Tel:  
44-141 548 2659)

**ABSTRACT**--We have assessed the effect of two ether glycerol lipids, **77-6** ((2*S*, 3*R*)-4-(Tetradecyloxy)-2-amino-1,3-butanediol) and **56-5** ((*S*)-2-Amino-3-*O*-hexadecyl-1-propanol), which are substrates for sphingosine kinases, on inflammatory responses. Treatment of differentiated U937 macrophage-like cells with **77-6** but not **56-5** enhanced IL-1 $\beta$  release; either alone or in the presence of LPS. The stimulatory effect of sphingosine or **77-6** on LPS-stimulated IL-1 $\beta$  release was reduced by pretreatment of cells with the caspase-1 inhibitor, Ac-YVAD-CHO, thereby indicating a role for the inflammasome. The enhancement of LPS-stimulated IL-1 $\beta$  release in response to sphingosine, but not **77-6**, was reduced by pretreatment of cells with the cathepsin B inhibitor, CA074Me, indicating a role for lysosomal destabilization in the effect of sphingosine. Administration of **56-5** to mice increased disease progression in an experimental autoimmune encephalomyelitis model and this was associated with a considerable increase in the infiltration of CD4<sup>+</sup> T-cells, CD11b<sup>+</sup> monocytes and F4/80<sup>+</sup> macrophages in the spinal cord. **56-5** and **77-6** were without effect on the degradation of myc-tagged sphingosine 1-phosphate 1 receptor in CCL39 cells. Therefore, the effect of **56-5** on EAE disease progression is likely to be independent of the inflammasome or the sphingosine 1-phosphate 1 receptor. However, **56-5** is chemically similar to platelet activating factor and the exacerbation of EAE disease progression might be linked to platelet activating factor receptor signaling.

## Introduction

Innate immunity to pathogens uses pathogen-associated molecular patterns (PAMPs) to increase IL-1 $\beta$  and IL-18 release from inflammatory cells (Schroder & Tschopp, 2010). Lipopolysaccharide (LPS) is an example of a PAMP that can bind to Toll-Like Receptors (TLR) to initiate innate immune responses (Takeuchi & Akira, 2010). In addition, during sterile inflammation, danger-associated molecular patterns (DAMPs) can be released from dead cells to promote innate immune responses via TLR-dependent pathways (Chen & Nunez, 2010). The NLRP (NOD-like receptor family, pyrin domain containing) inflammasome senses DAMPs, resulting in the binding of apoptosis-associated speck-like protein containing a caspase recruitment domain (ASC) to the inflammasome. This, in turn, promotes assembly and activation of caspase-1, which cleaves pro-IL-1 $\beta$  to produce bioactive IL-1 $\beta$  which is then released from cells (Brough & Rothwell, 2007). DAMPs might also be released from the damage to lysosomal membranes, which is regulated by lysosomal proteases, such as cathepsin B (Hornung & Latz, 2010). Recently, Luheshi et al. (2012) demonstrated that sphingosine and the sphingosine analogue, FTY720, promote the NLRP3-dependent release of IL-1 $\beta$  from LPS-stimulated macrophages, as this was not evident in macrophages derived from *Nlrp3*<sup>-/-</sup> mice. The effect of sphingosine on IL-1 $\beta$  release involves the protein phosphatase 2A and/or protein phosphatase 1 (PP2A/PP1). Thus, the PP2A/PP1 inhibitors okadaic acid and calyculin A prevented sphingosine-induced IL-1 $\beta$  release from macrophages (Luheshi et al. 2012). Moreover, sphingosine-induced IL-1 $\beta$  release was

unaffected by the cathepsin B inhibitor, CA074Me, or the pan-cysteine protease inhibitor, E64 (Luheshi et al. 2012). The possibility that the effect of sphingosine on NLRP3-dependent release of IL-1 $\beta$  is mediated through metabolites of sphingosine was excluded based on the finding that ceramide, which is formed by acylation of sphingosine (catalysed by ceramidase and/or ceramide synthase) had no effect on IL-1 $\beta$  release. Moreover, much higher concentrations of sphingosine 1-phosphate (compared with sphingosine), which is produced by phosphorylation of sphingosine by the action of sphingosine kinase (two isoforms termed SK1 and SK2), were required in order to stimulate IL-1 $\beta$  release (Luheshi et al. 2012). These findings can possibly be explained by evidence showing that sphingosine potently binds to the acidic leucine rich nuclear phosphoprotein-32A (ANP32A) to activate PP2A (Habrukowich et al. 2010), and that this might also underlie the ability of sphingosine to inhibit cell growth and induce apoptosis of mammalian cells (Ohta et al. 1995; Nava et al. 2000) and to reduce tumour growth *in vivo* (Kohno et al. 2006).

Multiple sclerosis is an autoimmune inflammatory demyelinating disease involving reactive T-lymphocytes. There is also a strong prognostic relationship between IL-1 $\beta$  levels and disease progression and mutation of the *Nlrp3* gene is associated with MS-like lesions (Compeyrot-Lacassagne et al. 2009; Dodé, et al. 2002). In addition, mice lacking the gene encoding NLRP3 (*Nlrp3*<sup>-/-</sup>) develop significantly milder symptoms in an experimental autoimmune encephalomyelitis (EAE) model and exhibit a reduction in IFN $\gamma$ - and IL-17-expressing TH cells in peripheral lymphoid tissues and the spinal cord (Gris et al. 2010; Inoue et al. 2012). IL-1 $\beta$  also induces activation of microglial cells, which stimulate T-lymphocytes with self-antigen during EAE development. In addition, IL-1 receptor deficient mice develop milder EAE and reduced TH17 cells (Sutton et al. 2006). There is also a relationship between multiple sclerosis, NLRP3 inflammasome and the sphingosine analogue, FTY720. Indeed, FTY720 has been shown to activate PP2A, to stimulate IL- $\beta$  release via an NLRP3-dependent mechanism in macrophages (Luheshi et al. 2012) and to modulate the immune response by preventing egress of T-lymphocytes from lymph nodes (Hla & Brinkmann, 2011). FTY720 is licenced for oral treatment of relapsing multiple sclerosis under the trade name Gilenya<sup>TM</sup>. FTY720 is a prodrug, which is phosphorylated by SK2 and is a functional antagonist of sphingosine 1-phosphate receptor 1 (S1P<sub>1</sub>), causing this receptor to be degraded by the proteasome and removed from T-lymphocytes (Hla & Brinkmann, 2011). Since T-lymphocytes use an S1P gradient to egress from lymph nodes,

FTY720 is able to prevent this by creating S1P<sub>1</sub> null T-lymphocytes that do not respond to the S1P gradient. This traps the T-lymphocytes in lymph nodes, thereby preventing their action on the CNS in multiple sclerosis.

In the current study, we have assessed whether ether glycerol lipids can affect inflammasome-dependent IL-1 $\beta$  release from macrophages and modify disease progression in the EAE model. The rationale for this was three-fold. First, there is structural similarity of the ether glycerol lipids with sphingosine and therefore these molecules might act in a similar manner as sphingosine to modulate inflammasome-dependent IL-1 $\beta$  release. Second, if modulation of inflammasome-dependent IL-1 $\beta$  release is evident, then these ether glycerol lipids might serve as a starting point for the synthesis of potent inhibitors of the inflammasome that can be used therapeutically to abrogate inflammatory diseases. Alternatively, the synthesis of potent inflammasome activators could be used promote innate immunity against invading pathogens. Third, previous studies using 1-*O*-hexadecyl-2-desoxy-2-amino-*sn*-glycerol (which is **56-5**) have demonstrated its phosphorylation by SK1 ( $K_m = 3.8 \mu\text{M}$ , compared with  $K_m = 15.7 \mu\text{M}$  for sphingosine (sphing-4-enine) (Gijsbers et al. 2002). Indeed, we show here that ether glycerol lipids are substrates for SK1 and SK2, and that **77-6** is a powerful stimulator of IL-1 $\beta$  release from macrophages. However, **56-5** which fails to stimulate IL-1 $\beta$  release in U937 macrophage-like cells, increases disease progression in the EAE model. This action of **56-5** might be related to its chemical similarity with platelet activating factor, which also has a role in multiple sclerosis (Kihara et al. 2005).

## Results and Discussion

**77-6** and **56-5** are substrates for both SK1 and SK2--We assessed whether several ether glycerol lipids (**56-2**, **56-3**, **56-4**, **56-5**, **77-5** and **77-6**; Fig. 1) and a sphingosine analogue (**67-622**, Fig. 1) inhibit SK1 and SK2 activity and/or function as substrates for these enzymes (Table 1). The replacement of the azide group in **56-4**; a compound which inhibited SK2 activity, with an -NH<sub>2</sub> group produced compound **56-5** ((*S*)-2-Amino-3-*O*-hexadecyl-1-propanol or 1-*O*-hexadecyl-2-desoxy-2-amino-*sn*-glycerol), which was a substrate for SK2 (Table 1). **56-5** was also a weak substrate for SK1, being ~ 5 times less effective than for SK2 (Table 1). Similarly, replacement of the azide in **77-5** with an -NH<sub>2</sub> group produced compound **77-6** ((2*S*, 3*R*)-4-(Tetradecyloxy)-2-amino-1,3-butanediol), which was a substrate for SK2; this being ~ 3 times as effective compared with **56-5** (Table 1). Therefore, reduction

in the alkyl chain length from C16 to C14 and introduction of the 3-hydroxyl group, enhanced substrate utilization by SK2. Indeed, the 3-hydroxyl group of the naturally occurring substrate of SK2, sphingosine, might H-bond with D308 to orientate the 1-hydroxyl group for phosphorylation by the enzyme. **77-6** was also a preferred substrate for SK1 compared with **56-5**. **56-5** and **77-6** bear chemical resemblance with sphingoid bases and this might therefore provide explanation for why these molecules can function as substrates for both SK1 and SK2. Indeed, the effect of carbon alkyl chain length on the efficiency of phosphorylation suggests an optimal fit in the catalytic site of both SK1 and SK2 in terms of the positioning the –OH group in the sphingosine binding pocket close to the deprotonating base to enable efficient phosphorylation. In contrast, the sphingosine analogue, **67-622** was a selective inhibitor of SK1 with no inhibitor activity against SK2 (Table 1). **67-622** was not a substrate for SK1 or SK2 (Table 1).

*Effect of 77-6 and 56-5 on IL-1 $\beta$  release*--Others have shown that sphingosine stimulates IL-1 $\beta$  release from macrophages via activation of the NLRP3 inflammasome (Luheshi et al. 2012). Therefore, given the chemical similarity with sphingosine, we investigated the effect of **56-5** and **77-6** on IL-1 $\beta$  release from macrophages. We show here that treatment of differentiated (macrophage-like) U937 cells with **77-6** (10  $\mu$ M) increased basal and LPS-stimulated IL-1 $\beta$  release in differentiated U937 cells (Fig. 2A, B). Similarly, treatment of differentiated U937 cells with sphingosine enhanced LPS-stimulated IL-1 $\beta$  release (Fig. 3). In contrast, **56-5** (10  $\mu$ M) was ineffective in stimulating IL-1 $\beta$  release from these cells; either alone or in the presence of LPS (Fig. 2A, B). Thus, the presence of the 3–OH group and/or C14 alkyl chain length (2 carbons shorter than in **56-5**) in **77-6** is required to stimulate IL-1 $\beta$  release from macrophages suggesting some structural-activity relationship with respect to the modulation of inflammasome activity.

In order to exclude the possibility that potential metabolites of sphingosine are responsible for its effects on IL-1 $\beta$  release, we tested S1P, which is formed by the action of sphingosine kinase on sphingosine. We also tested the effect of short chain ceramides. S1P and short chain ceramides and the SK2 selective inhibitor, (*R*)-FTY720 methylether (ROME) (Lim et al. 2011b) had no effect on LPS-stimulated IL-1 $\beta$  release (Fig. 4). Similarly, the SK1/2 inhibitor, SKi (2-(*p*-hydroxyanilino)-4-(*p*-chlorophenyl)thiazole) failed to modulate LPS-stimulated IL-1 $\beta$  release (data not shown). Taken together, these results suggest that the effect of **77-6** (Fig.

2) is not via modulation of the sphingolipid rheostat (e.g. inter-conversion of ceramide, sphingosine and S1P). Neither sphingosine, **56-5** nor **77-6** affected basal or LPS-stimulated TNF $\alpha$  release (data not shown), suggesting that the ability of **77-6** to increase IL-1 $\beta$  release is regulated by a distinct mechanism (e.g. inflammasome) from that regulating TNF $\alpha$  expression.

The effect of sphingosine or **77-6** on LPS-stimulated IL-1 $\beta$  release was reduced by pretreatment of cells with the caspase-1 inhibitor, Ac-YVAD-CHO (Fig. 5), thereby indicating a role for the inflammasome. LPS-stimulated IL-1 $\beta$  release in response to sphingosine, but not **77-6**, was reduced by pretreatment of cells with the cathepsin B inhibitor, CA074Me (Fig. 6), indicating a role for lysosomal destabilization in the effect of sphingosine, but not **77-6**. Treatment of cells with the PP2A inhibitor, okadaic acid (0.5  $\mu$ M) had no effect on the enhancement of LPS-stimulated IL-1 $\beta$  release by **77-6** or sphingosine (Fig. 7). Higher concentrations of okadaic acid (2  $\mu$ M) actually enhanced LPS-stimulated IL-1 $\beta$  formation (data not shown). These findings are different from those reported for primary macrophages, where okadaic acid reduced the effect of sphingosine on IL-1 $\beta$  release and CA074Me had no effect. There is a major difference in the response of U937 macrophage like cells and primary macrophages, as in the latter case, LPS alone has no effect on IL-1 $\beta$  release (Luheshi et al. 2012), while in U937 macrophage like cells, LPS alone is able to stimulate IL-1 $\beta$  release. These findings suggest that the mechanisms of LPS-stimulated IL-1 $\beta$  release are somewhat different in the two cell systems. Therefore, it is reasonable to conclude that the DAMP-mediated effect of sphingosine could also involve different mechanisms of inflammasome modulation in the two cellular systems. For instance, different family members of NLRP inflammasome might be involved in the two cell types. The effect of sphingosine, but not **77-6**, on LPS stimulation of IL-1 $\beta$  release was also reduced by the cyclic AMP elevating agent, forskolin (Fig. 8), thereby indicating along with the differential effect of cathepsin B inhibitor, that sphingosine and **77-6** use different mechanisms involving the inflammasome to potentiate LPS-stimulated IL-1 $\beta$  release from macrophages.

*Effect of 56-5 and 77-6 on disease progression in EAE*--Since the inflammasome is linked with multiple sclerosis, we tested the effect of **56-5** and **77-6** on disease progression in EAE, an animal model of multiple sclerosis. In this regard, **56-5** increased disease progression (clinical score) with an earlier onset of symptoms that were more severe (Fig. 9A) in the EAE

model and induced a considerable increase in infiltration in CD4<sup>+</sup> T-cells, CD11b<sup>+</sup> monocytes and F4/80<sup>+</sup> macrophages in the spinal cord (Fig. 9B). In contrast, **77-6** was without effect on disease progression (Fig. 9A B). FTY720, used as a positive control, completely ablated disease progression (clinical score) in the EAE model (Fig. 9A). These findings demonstrate the opposite structural-activity relationship when compared to the modulation of IL-1 $\beta$  release and suggest that the targets for **77-6** and **56-5** are different in the two experimental systems. The amino ether lipid **56-5** is an intermediate in the chemical synthesis of an amide analogue of PAF (1-*O*-alkyl-2-acetyl-*sn*-glycerol-3-phosphocholine) (Chandrakumar & Hadju, 1982) and bears some chemical similarity to PAF, which is also involved in disease progression in EAE. Indeed, PAF levels and PAF receptor mRNA expression in the spinal cord are correlated with the EAE disease progression. Moreover, PAF receptor knockout mice exhibit a lower incidence and less severe symptoms in the chronic phase of EAE compared with WT mice (Kihara et al. 2005). In addition, macrophages from PAF receptor knockout mice exhibit enhanced phagocytic activity and TNF- $\alpha$  production. Therefore, the ability of **56-5** to enhance disease progression in the EAE model might be related to its potential activity in modulating PAF receptor signaling. This possibility will be tested by further experimentation in the future.

*Effect of FTY720, 56-5 and 77-6 on S1P<sub>1</sub> receptor internalization*--Since FTY720, when converted by SK2 to FTY720-phosphate, is a functional antagonist of the S1P<sub>1</sub> receptor and this underlies a major part of its action in alleviating MS disease progression, we assessed the effect of **56-5** and **77-6** (both SK2 substrates) on S1P<sub>1</sub> receptor degradation in CCL39 cells (an expression system for analyzing S1P<sub>1</sub> receptor modifying agents) that were engineered to stably over-express S1P<sub>1</sub>. Unlike FTY720, which significantly reduced EAE severity and S1P<sub>1</sub> levels in CCL39 cells, **56-5** and **77-6** were without effect on the degradation of this receptor (Fig. 10), and also failed to stabilize the receptor as neither **56-5** nor **77-6** stimulated increased expression of S1P<sub>1</sub>. Therefore, it is unlikely that the effects of **56-5** on EAE progression involve modulation of the S1P<sub>1</sub> receptor or T-lymphocyte trafficking from lymph nodes via this mechanism (although this would need to be tested in T-cells themselves), despite increasing CD4<sup>+</sup> infiltration into the spinal cord.

## Conclusion

The ability of **56-5** to increase disease progression in the EAE model is not likely to be linked with the inflammasome based on the finding that **56-5** failed to increase IL-1 $\beta$  release from differentiated U937 cells; either alone or in the presence of LPS. Moreover, a significant role for inflammasome in the action of **77-6** is unlikely as although this compound does stimulate IL-1 $\beta$  release from macrophages, it had no significant effect on disease progression in the EAE model. Therefore, we have demonstrated a structural activity relationship in terms of regulation of the inflammasome and EAE disease progression by ether glycerol lipids, albeit that these relationships are opposed. The concentration of **77-6** used to modulate IL-1 $\beta$  release is moderate ( $\mu$ M), and future development is required in order to increase potency. If this can be achieved, then consideration could be given for the use of glycerol lipids, possibly as potential PAF antagonists, for use in multiple sclerosis or inhibitors of inflammasome activity. Clearly this would involve synthesis of compounds where stimulatory activity is switched to inhibitory activity by chemical design. The objective would be the development of antagonists that block, for instance, sphingosine-dependent activation of IL-1 $\beta$  release in inflammatory disease. Alternatively, activators of IL-1 $\beta$  release could be exploited to promote innate immunity against pathogens.

## **Materials and Methods**

*HEK 293, U937 and CCL39 Cell Culture*--HEK 293 cells stably over-expressing GFP-SK1 (30-fold increase in SK1 activity vs. vector-transfected cells) were cultured in DMEM supplemented with 10% European fetal calf serum, 100 U/mL penicillin, 100  $\mu$ g/mL streptomycin, 1% non-essential amino acids, and 0.8% geneticin at 37 °C in 5% CO<sub>2</sub>. U937 cells (ATCC) were maintained in RPMI medium (Life Technologies), supplemented with 10% (v/v) foetal bovine serum (Seralabs), 1U /ml penicillin, 1 mg/ml streptomycin and 2 mM L-glutamine (Life Technologies; complete RPMI). U937 cells were differentiated using PMA as previously described by others (Shepherd et al. 2004; Twomey et al. 1993). Briefly, cells were plated at  $1 \times 10^6$  cells/ml in complete RPMI supplemented with 4nM PMA. Medium was replenished after two days. After 4 days, the cells were then cultured in complete RPMI in the absence of PMA for a further 24 hours. U937 cells were stimulated with 1  $\mu$ g/ml LPS (Sigma) for 2 hours, after which compounds at indicated concentrations were added for 1 hour. Supernatants were collected and assayed for IL-1 $\beta$  protein expression by ELISA according to the manufacturer's instructions (R&D Systems). CCL39 cells that were stably transfected with myc-tagged S1P<sub>1</sub> (Rutherford et al., 2013) were maintained in DMEM with

GlutaMAX<sup>TM</sup> supplemented with 10% (v/v) foetal bovine serum, 100 units/ml penicillin and 100  $\mu$ g/ml streptomycin at 37°C in a humidified atmosphere containing 5% (v/v) CO<sub>2</sub>. Cells grown to confluence on 12 well plates were quiesced for 24 hours prior to treatment with FTY720 (100 nM) or **77-6** (10  $\mu$ M) or **56-5** (10  $\mu$ M) for 24 hours. Cell lysates were analysed by SDS-PAGE and western blotted for myc-tagged S1P<sub>1</sub> (# sc-40, Santa Cruz) and re-probed for ERK-2 (# 610104, Transduction Laboratories) to ensure equal protein loading. It is standard practice to differentiate U937 myeloid to macrophages to study inflammatory responses e.g. IL-1 $\beta$  release. HEK293 cells and CCL39 cells are used as standard for over-expression of recombinant proteins (in this case SK1 or S1P<sub>1</sub>) in order to allow testing of compounds for target engagement.

*Western Blotting*--Upon treatment, cells were lysed in sample buffer (62.5 mM Tris-HCl (pH 6.7), 0.5 M sodium pyrophosphate, 1.25 mM EDTA, 1.25% (w/v) sodium dodecyl sulphate, 0.06% (w/v) bromophenol blue, 12.5% (v/v) glycerol (all from Sigma) and 50 mM dithiothreitol (Enzo)). Proteins were separated on a 10% (v/v) acrylamide/bisacrylamide gel, and transferred to a nitrocellulose Hybond membrane (GE Healthcare). Membranes were blocked in 5% (w/v) BSA (Fisher) in TBST buffer (20mM Tris-HCl (pH 7.5), 48mM NaCl, 0.1% (v/v) Tween20) for 1 hour at room temperature prior to incubation with primary antibody (diluted in blocking buffer) overnight at 4°C. Following three washes in TBST, membranes were incubated with secondary antibody (Sigma; diluted in blocking buffer) for 1 hour at room temperature. Immunoreactive protein bands were visualized using ECL.

*Sphingosine Kinase Activity Assays*--To assess the compounds as potential inhibitors of SK1 and SK2, enzyme activity was assayed at the K<sub>m</sub> values for sphingosine (SK1, 3  $\mu$ M; SK2, 10  $\mu$ M). This corresponds to 50% substrate saturation, thereby enabling a qualitative estimation of selectivity by comparing the % modulation of each kinase using a fixed concentration of compound (50  $\mu$ M). In order to measure SK2 activity, Sph was complexed with fatty acid free bovine serum albumin (final concentration, 0.2 mg/mL) in buffer A containing 20 mM Tris (pH 7.4), 1 mM EDTA, 1 mM Na<sub>3</sub>VO<sub>4</sub>, 40 mM  $\beta$ -glycerophosphate, 1 mM NaF, 0.007% (v/v)  $\beta$ -mercaptoethanol, 20% (v/v) glycerol, 10  $\mu$ g/ml aprotinin, 10  $\mu$ g/mL soybean trypsin inhibitor, 1 mM PMSF, 0.5 mM 4-deoxypyridoxine, and 400 mM KCl. SK2 assays were performed using 37 ng of purified SK2 and incubating the assay for 30 min at 30 °C in the presence of 10  $\mu$ M Sph, 250  $\mu$ M [ $\gamma$ -<sup>32</sup>P]-ATP (Perkin Elmer) in 10 mM MgCl<sub>2</sub>, and varying concentrations of the

inhibitors dissolved in DMSO or control (5% v/v DMSO). To measure SK1 activity, Sph was solubilized in Triton X-100 (final concentration, 0.063% w/v) and combined with buffer A without KCl. 30 µg of recombinant SK1 was incubated for 30 min at 30 °C, in the presence of 3 µM Sph, 250 µM [ $\gamma$ -<sup>32</sup>P]-ATP in 10 mM MgCl<sub>2</sub> with or without inhibitor dissolved in DMSO or control (5% v/v DMSO). Both assay reactions were terminated by the addition of 500 µl of 1-butanol. After 1 ml of 2 M KCl was added, with mixing, two phases were formed. The lower (aqueous) phase, which contains unreacted [ $\gamma$ -<sup>32</sup>P]-ATP, was removed and discarded. The organic phase containing [<sup>32</sup>P]-S1P was extracted by washing twice with 2 M KCl (1 ml each time) before quantification by Cerenkov counting. To evaluate the test compounds as putative substrates of SK1 and SK2, the assay was conducted in the presence of 50 µM of the test compound (but in the absence of Sph) and radioactivity in the 1-butanol phase was quantified.

*Mice*--C57BL/6 mice were purchased from Harlan (UK) and maintained at the Biological Procedure Unit, University of Strathclyde. All experiments were performed under the guidelines of the UK Home Office Animals (Scientific Procedures) Act 1986. Female mice at the age of 7–12 weeks were used in all experiments.

*EAE Induction and Clinical Evaluation*--Mice were immunized subcutaneously on the back with 100 µg of MOG<sub>35-55</sub> peptide (Sigma Genosys) in 50 µl of PBS emulsified with an equal volume of CFA (total 125 µg of *Mycobacterium tuberculosis*, strain H37RA, Difco, Detroit MI) as before (Jiang et al., 2012). Each mouse also received intraperitoneally (i.p.) 100 ng/200 µl of PTX (Sigma, UK) in PBS on days 0 and 2 post immunization. EAE was scored according to a 0 - 5 scale as follows: 0, no clinical sign; 1, complete loss of tail tone; 2, hind limb weakness; 3, hind limb paralysis; 4, forelimb involvement; 5, moribund.

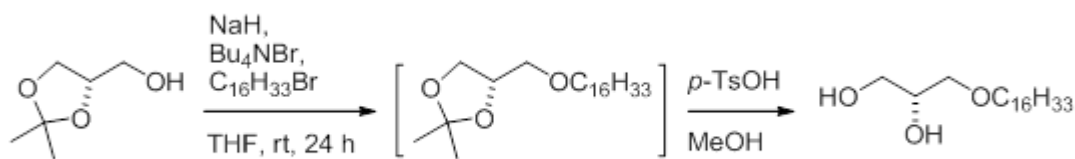
*Preparation of Compounds, Dosage and Route of Administration*--All compounds were dissolved in a vehicle solution of 20% cyclodextrin in phosphate buffered saline. FTY720 (Cambridge Bioscience, UK) was prepared as 0.05 mg/ml stock. The dosage given to the mice was 0.4 mg/kg. Compound **56-5** was prepared as 0.25 mg/ml stock. The dosage given was 2 mg/kg (the approximate *in vivo* concentration is 6.3 µM assuming 100% bioavailability). Compound **77-6** was prepared as 1.0 mg/ml stock. The dosage given was 8 mg/kg (the approximate *in vivo* concentration is 25 µM assuming 100% bioavailability). The compounds were all administered i.p. daily from day 0 of MOG immunization at the above doses. The EAE

control group received i.p. injection daily of the 20% cyclodextrin vehicle.

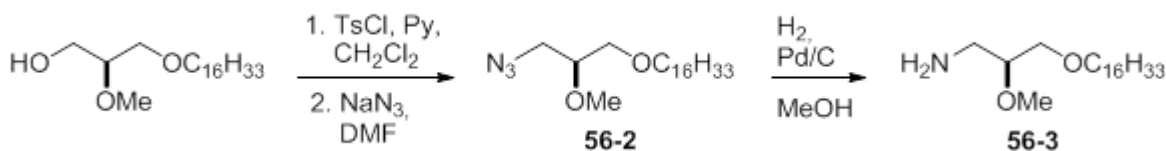
*Immunohistochemical Staining*--Mice were euthanized in CO<sub>2</sub> chamber and their spinal cords were flushed out with PBS by hydrostatic pressure using a syringe. Tissues were immediately frozen in OCT and 6-8µm thick sections were stained with specific primary antibodies for CD4, CD11b and F4/80 (all from e-Bioscience) overnight. Sections were then washed and incubated with biotinylated secondary antibody (Vector Laboratories) and streptavidin-HRP (eBioscience) before being detected with ImmPACT AMEC red peroxidase substrate (Vector Laboratories). Sections were then washed in distilled water and counterstained with haematoxylin. Isotypes with matching IgG were used as negative control and showed no staining in all tissues.

#### *Chemical Synthesis*

**3-*O*-Hexadecyl-*sn*-glycerol** (van Boeckel et al. 1982). To a suspension of 0.80 g (20.0 mmol) of sodium hydride (60% in white oil, washed with dry hexane twice) in 50 mL of dry THF was added 1.33 g (10.0 mmol) of 1,2-*O*-isopropylidene-*sn*-glycerol at 0 °C. After the evolution of hydrogen stopped, 3.1 mL (10.1 mmol) of *n*-hexadecyl bromide and 0.33 g (1.0 mmol) of *n*-Bu<sub>4</sub>NBr were added. The mixture was stirred for 24 h at room temperature, and then the reaction was quenched with 10 mL of methanol. The solvent was removed under reduced pressure and the residue was diluted with 100 mL of ether, and then washed with water. The organic layer was concentrated under reduced pressure. The residue was treated with 0.19 g (1.0 mmol) of *p*-toluenesulfonic acid (*p*-TsOH) in 50 mL of MeOH, and then was stirred overnight. Removal of the solvent gave a residue that was purified by column chromatography on silica gel (elution with hexane/EtOAc 1:1), affording 2.66 g (84%) of 3-*O*-hexadecyl-*sn*-glycerol as a white solid; mp 64.0-67.0 °C [63.0-64.0 °C];  $[\alpha]_D^{25} +2.69^\circ$  (*c* 5.0, THF)  $[[\alpha]_D^{25} +2.69^\circ$  (*c* 3.5, THF)]; <sup>1</sup>H NMR (CDCl<sub>3</sub>) δ 0.88 (t, 3H, *J* = 6.6 Hz), 1.26 (s, 26H), 1.50-1.60 (m, 2H), 2.55 (s, 2H), 3.44-3.49 (m, 4H), 3.50 (dd, 1H, *J* = 5.3, 11.3 Hz), 3.68 (dd, 1H, *J* = 5.3, 18.4 Hz), 3.80-3.90 (m, 1H); <sup>13</sup>C NMR δ 14.1, 22.7, 26.1, 29.3, 29.4, 29.6, 29.6, 29.6, 29.7, 31.9, 64.2, 70.5, 71.8, 72.5.

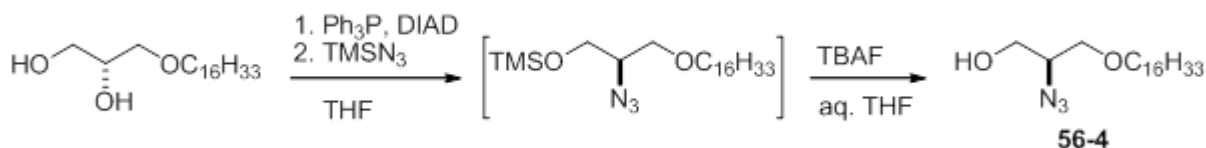


**(S)-3-Hexadecyloxy-2-methoxy-1-propylamine (56-3)** (Tsuru et al. 1992). 1-*O*-Hexadecyl-2-*O*-methyl-*sn*-glycerol was synthesized by *O*-methylation of 1-*O*-hexadecyl-3-*O*-(4-methoxyphenyl)-*sn*-glycerol as described previously (Byun et al. 1994). The azido group was introduced into the *sn*-3 position of 1-*O*-hexadecyl-2-*O*-methyl-*sn*-glycerol by using tosyl chloride followed by sodium azide as described previously. The azide group was reduced by hydrogenation of **56-2** (54 mg, 0.15 mmol) with Pd/C (5 mg) in methanol (20 mL), with stirring overnight. After Pd/C was removed by passing the mixture through a pad of Celite, the filtrate was concentrated under reduced pressure to give 50 mg of the target amino alcohol, **56-3**.

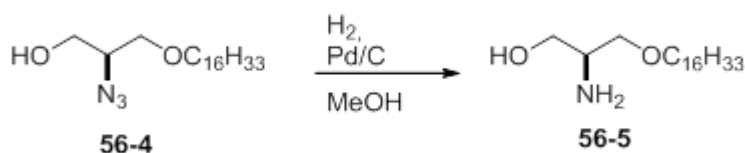


**(S)-2-Azido-3-*O*-hexadecyl-1,3-propanediol (56-4)** Regioselective azidotrimethylsilylation (Ponpipom & Bugianesi, 1984; He et al. 1999) of 3-*O*-hexadecyl-*sn*-glycerol was carried out as described previously (He et al. 1999; Byun et al. 2010). The activation of 3-*O*-hexadecyl-*sn*-glycerol (3.17 g, 10.0 mmol) with Ph<sub>3</sub>P (3.42 g, 13.0 mmol) and diisopropyl azodicarboxylate (DIAD, 3.2 mL, 15 mmol) followed by reaction with trimethylsilyl azide (TMSN<sub>3</sub>, 2.2 mL, 13 mmol) afforded crude the silyloxy azide, which was used without further purification. After removal silyl protecting group with tetra-*n*-butylammonium fluoride (TBAF, 25 mL of a 1 M solution in THF containing 5% H<sub>2</sub>O) the crude product was purified by silica gel chromatography (elution first with 150 mL of hexanes/EtOAc 50/1 and then with hexanes/EtOAc 6:1) to give 2.60 g (76%) of **56-4** as a white solid: mp 37-39 °C, 38-39 °C; 37-39 °C; [α]<sup>25</sup><sub>D</sub> +14.5° (c 1.0, CHCl<sub>3</sub>), [α]<sup>27</sup><sub>D</sub> +14.1° (c 1.0, CHCl<sub>3</sub>); [α]<sup>27</sup><sub>D</sub> +14.5° (c 1.0, CHCl<sub>3</sub>); <sup>1</sup>H NMR δ 0.86 (t, 3H, *J* = 7.0 Hz), 1.23 (m, 26H), 1.54 (m, 2H), 1.91 (br s, 1H), 3.45

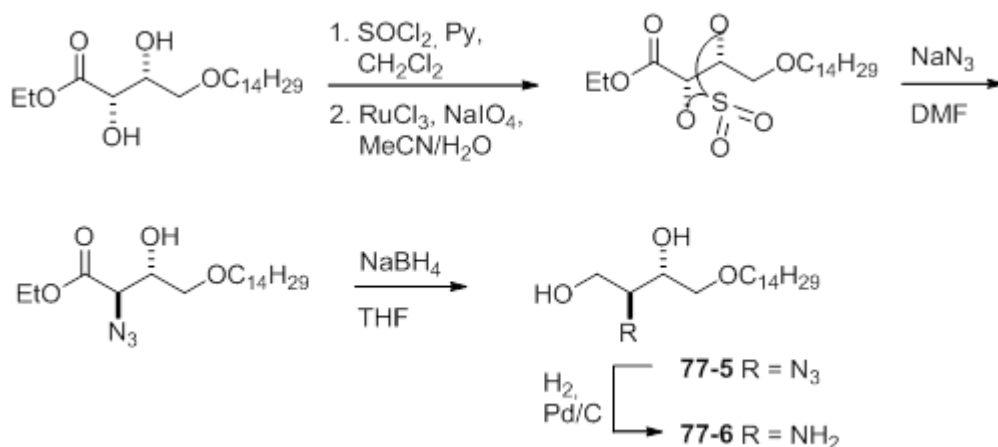
(dt, 2H,  $J = 6.6, 1.5$  Hz), 3.58-3.75 (m, 5H);  $^{13}\text{C}$  NMR  $\delta$  14.10, 22.68, 25.97, 29.35, 29.41, 29.56, 29.59, 29.65, 29.68, 31.91, 62.18, 63.09, 71.01, 71.91.



**(S)-2-Amino-3-O-hexadecyl-1,3-propanediol (56-5)** (Gijsbers et al. 2002). A mixture of azide **56-4** (103 mg, 0.30 mmol) and Pd/C (10 mg) in 20 mL of methanol was stirred overnight under a hydrogen atmosphere. After Pd/C was removed by passing the mixture through a pad of Celite, the filtrate was concentrated under reduced pressure to give 95 mg (100%) of the target 2-amino alcohol, **56-5**;  $^1\text{H}$  NMR ( $\text{CDCl}_3$ )  $\delta$  0.88 (t, 3H,  $J = 6.6$  Hz), 1.25 (m, 26H), 1.56 (q, 2H,  $J = 7.0$  Hz), 3.37-3.43 (m, 4H), 3.44-3.54 (m, 1H), 3.60-3.64 (m, 1H);  $^{13}\text{C}$  NMR  $\delta$  14.1, 22.7, 26.1, 29.3, 29.46, 29.50, 29.58, 29.61, 29.65, 29.68, 31.9, 52.1, 65.0, 71.7, 73.8.

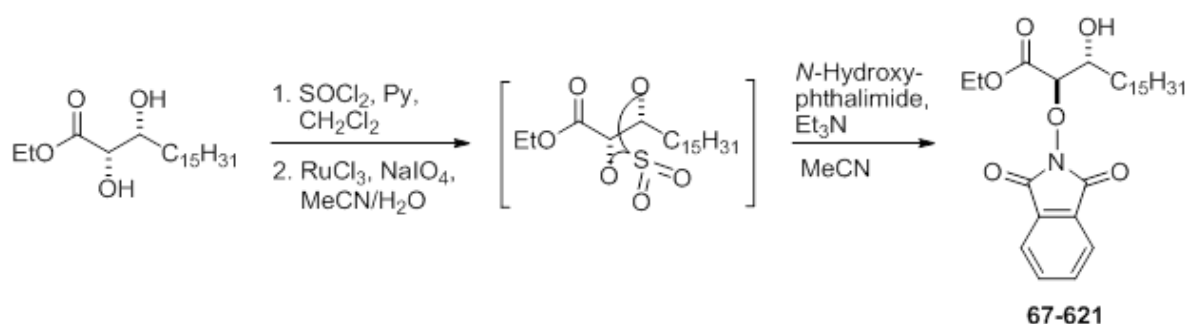


**(2S,3R)-4-(Tetradecyloxy)-2-amino-1,3-butanediol (77-6)**. Ethyl (2S,3R)-4-tetradecyloxy-2-azido-3-hydroxybutanone was prepared by asymmetric dihydroxylation (He et al. 2000) and converted to (2S,3R)-4-(tetradecyloxy)-2-azido-1,3-butanediol (**77-5**) as described previously (Byun et al. 2013). The azido group was reduced by hydrogenation with Pd/C in methanol, giving **77-6**;  $^1\text{H}$  NMR ( $\text{CDCl}_3$ )  $\delta$  0.88 (t,  $J = 6.7$  Hz, 3H), 1.26 (s, 22H), 1.54-1.61 (m, 2H), 2.48 (br s, 3H), 2.93 (br s, 1H), 3.42-3.52 (m, 4H), 3.56 (dd,  $J = 4.5, 9.7$  Hz, 1H), 3.61-3.69 (m, 2H), 3.70-3.76 (m, 1H);  $^{13}\text{C}$  NMR ( $\text{CDCl}_3$ )  $\delta$  14.1, 22.7, 26.1, 29.3, 29.44, 29.49, 29.56, 29.59, 29.6, 29.6, 31.9, 54.3, 64.4, 71.8, 72.0, 72.5.

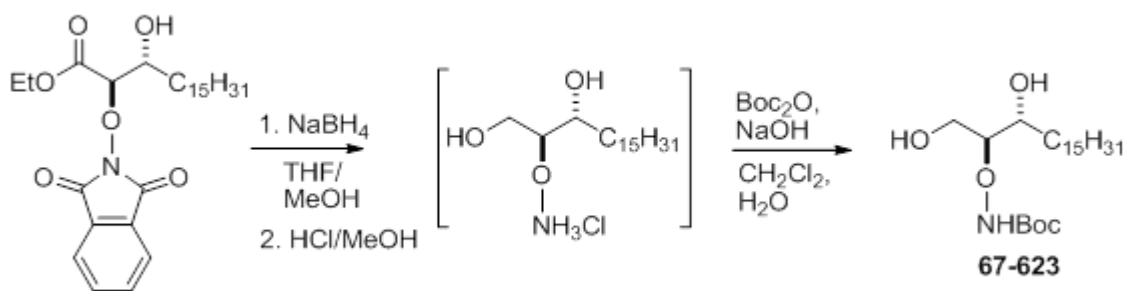


**Ethyl (2*S*,3*R*)-2-(*O*-Phthalimido-oxy)-3-hydroxyoctadecanoate (67-621).** To a solution of ethyl (2*S*,3*R*)-2,3-dihydroxyoctadecanoate (Byun et al. 2013) (345 mg, 1.0 mmol) in 30 mL of dry  $\text{CH}_2\text{Cl}_2$  was added 240  $\mu\text{L}$  (3.0 mmol) of pyridine at room temperature. After the mixture was stirred and chilled to 0 °C, 110  $\mu\text{L}$  (3.0 mmol) of  $\text{SOCl}_2$  was added slowly. The reaction mixture was stirred for 30 min, and then was filtered through a pad of silica gel in a sintered glass funnel. After the pad was washed with 100 mL of hexane/EtOAc (4:1), the filtrate was concentrated and further dried on a vacuum pump (1 h). The crude sulfite intermediate was used in the subsequent oxidation without further purification. To a solution of the crude cyclic sulfite in 20 mL of MeCN was added 321 mg (1.5 mmol) of  $\text{NaIO}_4$ . The heterogeneous mixture was stirred vigorously while 4 mg (0.010 mmol) of  $\text{RuCl}_3 \cdot 3\text{H}_2\text{O}$  in 4 mL of  $\text{H}_2\text{O}$  was added quickly. The reaction mixture was stirred at room temperature about 30 min. On addition of  $\text{Et}_2\text{O}$  (60 mL) to quench the reaction, the reaction mixture separated into two layers. After the top light brown clear solution was separated from the bottom slurry, a minimum volume of  $\text{H}_2\text{O}$  was added to dissolve the slurry. The aqueous phase was extracted with  $\text{Et}_2\text{O}$  (2 x 60 mL). The organic phases were combined, dried ( $\text{Na}_2\text{SO}_4$ ), and passed through a small pad of silica gel in order to remove the black color. Concentration of the filtrate followed by drying under vacuum gave the crude cyclic sulfate. To a solution of *N*-hydroxyphthalimide (213 mg, 1.30 mmol) and  $\text{Et}_3\text{N}$  (132 mg, 1.30 mmol) in 30 mL of MeCN was added a solution of crude cyclic sulfate in 10 mL of MeCN. The reaction mixture was stirred overnight at room temperature. Most of the acetonitrile was removed on a rotary evaporator, and the residue was dried by high vacuum (0.8 Torr). Then  $\text{Et}_2\text{O}$  (100 mL) and 20% aqueous  $\text{H}_2\text{SO}_4$  (50 mL) were added, and the heterogeneous mixture was stirred vigorously at room temperature until the hydrolysis was completed. The layers were separated, and the aqueous layer was extracted

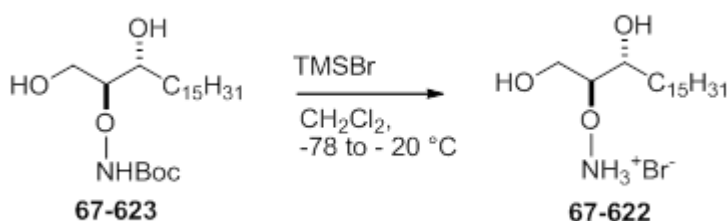
with Et<sub>2</sub>O (2 X 100 mL). Anhydrous K<sub>2</sub>CO<sub>3</sub> (100 mg) was added to the combined organic phase to remove the dissolved H<sub>2</sub>SO<sub>4</sub>. The ether solution was dried (Na<sub>2</sub>SO<sub>4</sub>), filtered through a small pad of silica gel in a sintered glass funnel, and concentrated to give a residue. The product was purified by column chromatography on silica gel (elution with hexane/EtOAc 2:1) to give 374 mg (76%) of **67-621**; <sup>1</sup>H NMR (CDCl<sub>3</sub>) δ 0.88 (t, 3H, *J* = 6.6 Hz), 1.26 (m, 26H), 1.33 (t, 3H, *J* = 7.2 Hz), 3.39 (br s, 1H), 4.05(dt, 1H, *J* = 3.5, 8.9 Hz), 4.25-4.38 (m, 2H), 4.65 (d, 1H, *J* = 3.5 Hz), 7.79 (dd, 2H, *J* = 3.1, 5.5 Hz), 7.86 (dd, 2H, *J* = 3.1, 5.5 Hz); <sup>13</sup>C NMR (CDCl<sub>3</sub>) δ 14.1, 22.7, 25.9, 29.3, 29.44, 29.48, 29.54, 29.63, 29.65, 29.67, 31.8, 31.9, 61.8, 70.6, 88.7, 123.9, 128.6, 134.9, 163.7, 166.9; HRMS (M + Na)<sup>+</sup>, calculated for C<sub>28</sub>H<sub>43</sub>NNaO<sub>6</sub> 512.2983, found 512.2983.



**(2*S*,3*R*)-2-*O*-(*tert*-Butoxycarbonylamido-oxy)-octadecane-1,3-diol (67-623).** To a solution of 184 mg (0.375 mmol) of **67-621** in 50 mL of THF was added 52 mg (1.34 mmol) of NaBH<sub>4</sub>, followed by 50 μL of MeOH at 0 °C. The reaction mixture was stirred vigorously and allowed to warm to room temperature. To the reaction mixture were added 1 mL of aqueous 1 M HCl solution and 100 mL of MeOH. The solvents were removed to give a residue. To the residue were added 1.1 g (1.51 mmol) of Boc<sub>2</sub>O (*ca.* 30% in toluene solution), 20 mL of CH<sub>2</sub>Cl<sub>2</sub>, and 5 mL of aqueous 1 M NaOH solution. After 24 h, the mixture was diluted with 100 mL of CH<sub>2</sub>Cl<sub>2</sub>, and washed with brine and water. The organic layer was dried (Na<sub>2</sub>SO<sub>4</sub>) and concentrated. The product was purified by column chromatography on silica gel (elution with hexane/EtOAc 1:1) to give 85 mg (51%) of **67-623**; <sup>1</sup>H NMR (CDCl<sub>3</sub>) δ 0.88 (t, 3H, *J* = 6.6 Hz), 1.49 (s, 9H), 1.46-1.54 (m, 2H), 1.77 (br s, 1H), 3.60-3.67 (m, 2H), 3.77-3.94 (m, 3H), 7.50 (s, 1H); <sup>13</sup>C NMR (CDCl<sub>3</sub>) δ 14.1, 22.7, 26.1, 28.1, 29.4, 29.57, 29.62, 29.66, 29.7, 31.9, 32.8, 59.9, 70.2, 83.0, 88.9, 158.9; HRMS (M + Na)<sup>+</sup>, calculated for C<sub>23</sub>H<sub>47</sub>NNaO<sub>5</sub><sup>+</sup> 440.3346, found 440.3343.



**(2*S*,3*R*)-2-*O*-(Aminooxy)-octadecane-1,3-diol Hydrobromide Salt (67-622).** To a solution of **67-623** (76 mg, 0.18 mmol) in 5 mL of CH<sub>2</sub>Cl<sub>2</sub> was added 150 μL (1.1 mmol) of TMSBr at -78 °C. The mixture had been stirred for 3 h at -78 °C, and then was kept at -20 °C overnight. After the solvents were removed, the residue was dissolved in 10 mL of 95% MeOH with stirring for 1 h. Removal of the solvent afforded 73 mg (100%) of **67-622** (hydrobromide salt); <sup>1</sup>H NMR (CDCl<sub>3</sub>/CD<sub>3</sub>OD) δ 0.89 (t, 3H, *J* = 6.6 Hz), 1.27 (m, 26H), 1.41-1.74 (m, 2H), 3.61-4.22(m, 4H); <sup>13</sup>C NMR (CDCl<sub>3</sub>/CD<sub>3</sub>OD) δ 13.81, 22.4, 25.5, 29.1, 29.29, 29.36, 29.40, 29.45, 31.6, 61.0, 70.4, 87.6; HRMS (M + H)<sup>+</sup>, calculated for C<sub>18</sub>H<sub>40</sub>NO<sub>3</sub><sup>+</sup> 318.3003, found 318.3005. The free amine was found to be unstable.



## References

- Brough, D., Rothwell, N.J. (2007) Caspase-1-dependent processing of prointerleukin-1 beta is cytosolic and precedes cell death. *J. Cell Sci.* 120, 772-781.
- Byun, H.-S., Bittman, R., Samadder, P., Arthur, G. (2010) Synthesis and antitumor activity of ether glycerophospholipids bearing a carbamate moiety at the *sn*-2 position: Selective sensitivity against prostate cancer cell lines. *ChemMedChem* 5, 1045-1052.
- Byun, H.-S., Kumar, E. R., Bittman, R. (1994) Enantioselective syntheses of 1-*O*-benzyl-*sn*-glycerol and 1-*O*-hexadecyl-2-*O*-methyl-*sn*-glycerol via asymmetric dihydroxylation of allyl 4-methoxyphenyl ether. Use of AD-mix supplemented with potassium persulfate. *J. Org. Chem.* 59, 2630-2633.
- Byun, H.-S., Pyne, S., MacRitchie, N., Pyne, N. J., Bittman, R. (2013) Novel sphingosine-containing analogues selectively inhibit sphingosine kinase (SK) isozymes, induce

SK1 proteasomal degradation and reduce DNA synthesis in human pulmonary arterial smooth muscle cells. *Med. Chem. Comm.* 4, 1394-1399.

Chandrakumar NS, Boyd VL, Hajdu J. (1982) Synthesis of enzyme-inhibitory phospholipid analogs. III. A facile synthesis of N-acylaminoethylphosphorylcholines. *Biochim Biophys Acta.* 711, 357-60.

Compeyrot-Lacassagne, S., Tran, T.A., Guillaume-Czitrom, S., Marie, I., Koné-Paut, I. (2009) Brain multiple sclerosis-like lesions in a patient with Muckle-Wells syndrome. *Rheumatology* 48, 1618–1619.

Chen, G.Y., Nunez, G. (2010) Sterile inflammation: sensing and reacting to damage. *Nat. Rev. Immunol.* 10, 826-837.

Dodé, C., Le Dû, N., Cuisset, L., Letourneur, F., Berthelot, J.M., Vaudour, G., Meyrier, A., Watts, R.A., Scott, D.G., Nicholls, A., Granel, B., Frances, C., Garcier, F., Edery, P., Boulinguez, S., Domergues, J.P., Delpech, M., Grateau, G. (2002) New mutations of CIAS1 that are responsible for Muckle-Wells syndrome and familial cold urticaria: a novel mutation underlies both syndromes. *Am. J. Hum. Gen.* 70, 1498-1506.

Gijsbers, S., Asselberghs, S., Herdewijn, P., Van Veldhoven, P.P. (2002) 1-O-Hexadecyl-2-desoxy-2-amino-sn-glycerol, a substrate for human sphingosine kinase. *Biochim. Biophys. Acta.* 1580, 1-8.

Gris, D., Ye, Z., Iocca, H.A., Wen, H., Craven, R.R., Gris, P., Huang, M., Schneider, M., Miller, S.D., Ting, J.P. (2010) NLRP3 plays a critical role in the development of experimental autoimmune encephalomyelitis by mediating Th1 and Th17 responses. *J. Immunol.* 185, 974–981.

Habrukowich, C., Han, D.K., Le, A., Rezaul, K., Pan, W., Ghosh, M., Li, Z., Dodge-Kafka, K., Jiang, X., Bittman, R., Hla, T. (2010) Sphingosine interaction with acidic leucine-rich nuclear phosphoprotein-32A (ANP32A) regulates PP2A activity and cyclooxygenase (COX)-2 expression in human endothelial cells. *J. Biol. Chem.* 285, 26825-26831.

He, L. Byun, H.-S., Bittman, R. (2000) A Stereocontrolled, Efficient Synthetic Route to Bioactive Sphingolipids: Synthesis of Phytosphingosine and Phytoceramides from Unsaturated Ester Precursors via Cyclic Sulfate Intermediates. *J. Org. Chem.* 65, 7618-7626.

He, L.; Wanunu, M., Byun, H.-S., Bittman, R. (1999) Regioselective and stereospecific azidation of 1,2- and 1,3-diols by azidotrimethylsilane via a Mitsunobu reaction. *J. Org. Chem.* 64, 6049-6055.

Hla, T., Brinkmann, V. (2011) Sphingosine 1-phosphate (S1P): Physiology and the effects of S1P receptor modulation. *Neurology.* 76, S3-8.

Hornung, V., Latz, E. (2010) Critical functions of priming and lysosomal damage for NLRP3 activation. *Eur. J. Immunol.* 40, 620-623.

Inoue, M., Williams, K.L., Gunn, M.D., Shinohara, M.L. (2012) NLRP3 inflammasome induces chemotactic immune cell migration to the CNS in experimental autoimmune Encephalomyelitis. *Proc. Natl. Acad. Sci.* 109, 10480-10485.

Jiang, H.R., Milovanović, M., Allan, D., Niedbala, W., Besnard, A.G., Fukada, S.Y., Alves-Filho, J.C., Togbe, D., Goodyear, C.S., Linington, C., Xu, D., Lukic, M.L., Liew, F.Y. (2012) IL-33 attenuates EAE by suppressing IL-17 and IFN- $\gamma$  production and inducing alternatively activated macrophages. *Eur. J. Immunol.* 42, 1804-1814.

Kihara, Y., Ishii, S., Kita, Y., Toda, A., Shimada, A., Shimizu, T. (2005) Dual phase regulation of experimental allergic encephalomyelitis by platelet-activating factor. *J. Exp. Med.* 202, 853-863.

Kohno, M., Momoi, M., Oo, M. L., Paik, J. H., Lee, Y. M., Venkataraman, K., Ai, Y., Ristimaki, A. P., Fyrst, H., Sano, H., Rosenberg, D., Saba, J. D., Proia, R. L., and Hla, T. (2006) Intracellular role for sphingosine kinase 1 in intestinal adenoma cell proliferation *Mol. Cell. Biol.* 26, 7211-7223.

Lim, K.G., Tonelli, F., Li, Z., Lu, X., Bittman, R., Pyne, S. & Pyne, N.J. (2011a) FTY720 analogues as sphingosine kinase 1 inhibitors: Enzyme inhibition kinetics, allosterism, proteasomal degradation and actin rearrangement in MCF-7 breast cancer cells. *J. Biol. Chem.* 286, 18633-18640.

Lim, K.G., Sun, C., Bittman, R., Pyne, N.J. & Pyne, S. (2011b) (R)-FTY720 methyl ether is a specific sphingosine kinase 2 inhibitor: effect on sphingosine kinase 2 expression in HEK 293 cells and actin rearrangement and survival of MCF-7 breast cancer cells. *Cell. Signal.* 23, 1590-1595

Luheshi, N.M., Giles, J.A., Lopez-Castejon, G., Brough, D. (2012) Sphingosine regulates the NLRP3 inflammasome and IL-1 $\beta$  release from macrophages. *Eur. J. Immunol.* 42, 716-725.

Nava, V. E., Cuvillier, O., Edsall, L. C., Kimura, K., Milstien, S., Gelmann, E. P., and Spiegel, S. (2000) Sphingosine enhances apoptosis of radiation-resistant prostate cancer cells. *Cancer Res.* 60, 4468-4474.

Ohta, H., Sweeney, E. A., Masamune, A., Yatomi, Y., Hakomori, S., and Igarashi, Y. (1995) Induction of apoptosis by sphingosine in human leukemic HL-60 cells: a possible endogenous modulator of apoptotic DNA fragmentation occurring during phorbol ester-induced differentiation. *Cancer Res.* 55, 691-697.

Ponpipom, M.M., Bugianesi, R.L. (1984) Synthesis of azide and amide analogs of platelet-activating factor and related derivatives. *Chem. Phys. Lipids* 35, 29-37.

Rutherford, C., Childs, S., Ohotski, J., McGlynn, L., Riddick, M., MacFarlane, S., Tasker, D., Pyne, S., Pyne, N.J., Edwards, J. & Palmer T.M. (2013) Regulation of cell survival by sphingosine 1-phosphate receptor 1 via reciprocal ERK-dependent suppression of BIM and PI-3-kinase/protein kinase C-mediated up-regulation of MCL-1. *Cell Death Dis.* 4, E927.

Schroder, K., Tschopp, J. (2010) The inflammasomes. *Cell* 140, 821-832.

Shepherd, M.C., Baillie, G.S., Stirling, D.I., Houslay, M.D. (2004) Remodelling of the PDE4 cAMP phosphodiesterase isoform profile upon monocyte-macrophage differentiation of human U937 cells. *Br. J. Pharmacol.* 142(2), 339-51.

Sutton, C., Brereton, C., Keogh, B., Mills, K.H.G., Lavelle, E.C. (2006) A crucial role for interleukin (IL)-1 in the induction of IL-17-producing T cells that mediate autoimmune encephalomyelitis. *J. Exp. Med.* 203, 1685–1691

Takeuchi, O., Akira, S. (2010) Pattern recognition receptors and inflammation. *Cell* 140, 805-820.

Tsuri, T., Haga, N., Matsui, T., Kamata, S., Kakushi, H., Uchida, K. (1992) A novel class of platelet activating factor (PAF) antagonists. I. Synthesis and structure-activity studies on PAF-sulfonamide isosteres. *Chem. Pharm. Bull.* 40, 75-84.

Twomey, B.M., McCallum, S., Isenberg, D.A., Latchman, D.S. (1993) Elevation of heat shock protein synthesis and hsp gene transcription during monocyte to macrophage differentiation of U937 cells. *Clin Exp Immunol.* 93, 178-183.

Weigert, A., Cremer, S., Schmidt, M.V., von Knethen, A., Angioni, C., Geisslinger, G., Brüne B. (2010) Cleavage of sphingosine kinase 2 by caspase-1 provokes its release from apoptotic cells. *Blood.* 115(17):3531-3540.

van Boeckel, C.A., van del Marel, G.A., Westerduin, P., van Boom, J.H. (1982) Synthesis of 2-*O*-acetyl-3-*O*-hexadecyl-*sn*-1-glycerolphosphorylcholine, the enantiomer of platelet-activating factor (PAF). *Synthesis* 5, 399-402.

## Figure legends

### **Figure 1. Chemical Structures**

**Figure 2. 77-6, but not 56-5 enhances IL-1 $\beta$  release in the presence and absence of LPS in differentiated U937 cells.** Differentiated U937 cells were treated with **56-5** (10  $\mu$ M) or **77-6** (10  $\mu$ M) for 1 hour (a) or stimulated with LPS (1  $\mu$ g/ml) for 2 hours and then treated with **56-5** (10  $\mu$ M) or **77-6** (10  $\mu$ M) for 1 hour (b), and the supernatants assayed for

IL-1 $\beta$  by ELISA. Data shown are the mean  $\pm$  SEM of at least 3 experiments. Student's T-test was carried out. \*\*\* $p$ <0.001.

**Figure 3. Sphingosine enhances IL-1 $\beta$  release in the presence of LPS in differentiated U937 cells.** Differentiated U937 cells were stimulated with LPS (1  $\mu$ g/ml) for 2 hours prior to treatment with sphingosine (Sph, 20  $\mu$ M) for 1 hour. The supernatants were collected and assayed for IL-1 $\beta$  by ELISA. Data shown are the mean  $\pm$  SEM of at least 3 experiments. Student's T-test was carried out. \*\*\* $p$ <0.001.

**Figure 4. S1P, C2 ceramide and ROME do not affect IL-1 $\beta$  release.** Differentiated U937 cells were stimulated with LPS (1  $\mu$ g/ml) for 2 hours prior to treatment with erythroS1P (1 and 10  $\mu$ M), C2 ceramide (10 and 50  $\mu$ M) or ROME (10  $\mu$ M) for 1 hour. The supernatants were collected and assayed for IL-1 $\beta$  by ELISA. Data shown are the mean  $\pm$  SEM of at least 3 experiments. Student's T-test was carried out. \*\*\* $p$ <0.001.

**Figure 5. The Caspase-1 inhibitor Ac-YVAD-CHO prevents the enhancement of LPS-stimulated IL-1 $\beta$  release by 77-6 and sphingosine.** Differentiated U937 cells were treated with vehicle (grey bars) or Ac-YVAD-CHO (10  $\mu$ M) for 15 min (black bars), stimulated with LPS (1  $\mu$ g/ml) for 2 hours prior to treatment with 56-5 or 77-6 (both at 10  $\mu$ M) or 20  $\mu$ M Sph for 1 hour. Data shown are the mean  $\pm$  SEM of at least 3 experiments. Student's T-test was carried out. \* $p$ <0.05, \*\* $p$ <0.01, ns not significant.

**Figure 6. The Cathepsin B inhibitor CA-074Me prevents the enhancement of LPS-stimulated IL-1 $\beta$  release by sphingosine but not 77-6.** Differentiated U937 cells were treated with vehicle (grey bars) or CA-074Me (10  $\mu$ M, black bars) for 15 min, stimulated with LPS (1  $\mu$ g/ml) for 2 hours prior to treatment with 56-5 or 77-6 (both at 10  $\mu$ M) or Sph (20  $\mu$ M) for 1 hour. Data shown are the mean  $\pm$  SEM of at least 3 experiments. Student's T-test was carried out. \* $p$ <0.05, \*\* $p$ <0.01, ns not significant.

**Figure 7. PP2A inhibitor okadaic acid does not affect IL-1 $\beta$  release.** Differentiated U937 cells were stimulated with LPS (1  $\mu$ g/ml) for 2 hours, treated with vehicle (grey bars) or okadaic acid (0.5  $\mu$ M) for 15 min (black bars), prior to treatment with 56-5 or 77-6 (both at 10  $\mu$ M) or 20  $\mu$ M Sph for 1 hour. Data shown are the mean  $\pm$  SEM of at least 3 experiments. Student's T-test was carried out. \* $p$ <0.05, \*\* $p$ <0.01, \*\*\* $p$ <0.001, ns not significant.

**Figure 8. Forskolin inhibits the enhancement of LPS-stimulated IL-1 $\beta$  release by sphingosine but not 77-6.** Differentiated U937 cells were treated with vehicle (grey bars) or Forskolin (10  $\mu$ M) for 30 min (black bars), stimulated with LPS (1  $\mu$ g/ml) for 2 hours prior to treatment with 56-5 or 77-6 (both at 10  $\mu$ M) or 20  $\mu$ M Sph for 1 hour. Data shown are the mean  $\pm$  SEM of at least 3 experiments. Student's T-test was carried out. \* $p$ <0.05, \*\* $p$ <0.01, ns not significant.

**Figure 9. The effect of 56-5, 77-6 or FTY720 on disease progression in EAE.** EAE-treated mice were dosed with FTY720 (0.4 mg/kg) or 56-5 (2mg/kg) or 77-6 (8 mg/kg). (A) Clinical scores are plotted against time and are represented as means  $\pm$  SEM for  $n$ =6 mice/treatment. (B) Immunohistochemical of spinal section with specific anti-CD4 or anti-CD11b or anti-F4/80 antibodies. Spinal sections from naïve mice are also shown stained with anti-CD4 or anti-CD11b or anti-F4/80 antibodies. Results are representative for  $n$ =6 animals/treatment group. Arrows denote infiltration of inflammatory cells.

**Figure 10. The effect 56-5, 77-6 or FTY720 on myc-tagged S1P<sub>1</sub> expression in CCL39 cells.** CCL39 cells stably over-expressing myc-tagged S1P<sub>1</sub> were treated with 56.5 (10  $\mu$ M) or 77-6 (10  $\mu$ M) or FTY720 (100 nM) for 24 h. Cell lysates were then western blotted with anti-myc antibodies. Results are representative of 3 independent experiments.

## ABBREVIATIONS

DAMPs, Danger associated molecular patterns; DMEM, Dulbeccos Modified Eagles Medium;

EAE, experimental autoimmune encephalomyelitis; ERK, extracellular signal regulated kinase; LPS, lipopolysaccharide; NLRP3, NOD-like receptor family, pyrin domain containing 3; IFN $\gamma$ , interferon gamma; IL-1 $\beta$ , interleukin-1beta; PAF, platelet activating factor; PAMPs, Pathogen-associated molecular patterns; PP2A, protein phosphatase 2A; PP1, protein phosphatase 1; SK, sphingosine kinase; S1P, sphingosine 1-phosphate; S1P<sub>1</sub>, sphingosine 1-phosphate receptor-1; TH, T helper cells; TLR, Toll-like receptors.

**Table 1***With sphingosine*

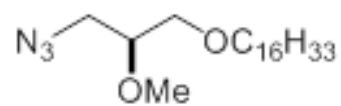
	<b>SK1</b>	<b>SK2</b>
Control	100 +/- 3.7	100 +/- 10
<b>56-2</b>	83.3 +/- 1.5	133.5 +/- 9.6
<b>56-3</b>	90.9 +/- 5.4	104.7 +/- 4
<b>56-4</b>	88.1 +/- 2.4	54.2 +/- 3.7
<b>56-5</b>	98.6 +/- 2.7	327.9 +/- 19.2
<b>77-5</b>	89.7 +/- 4.8	132.9 +/- 4.4
<b>77-6</b>	128 +/- 9.7	847.5 +/- 59.3
<b>67-622</b>	14.1 +/- 1.2	105 +/- 7.5

*Without sphingosine*

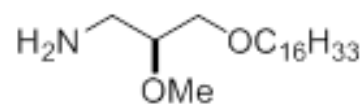
	<b>SK1</b>	<b>SK2</b>
<b>56-4</b>	9.4 +/- 1.6	11 +/- 1.1
<b>56-5</b>	42.4 +/- 0.3	251.8 +/- 14.9
<b>77-5</b>	8.1 +/- 8.5	23.9 +/- 1.4
<b>77-6</b>	88.2 +/- 2.7	822.6 +/- 50.2
<b>67-622</b>	0.8 +/- 1.2	21.9 +/- 1.3

SK1 and SK2 activity was measured according to the Methods. Compounds were tested in combination with sphingosine (control activity in assay with sphingosine alone =100%) or in the absence of sphingosine (activity in absence of compounds = 0%).

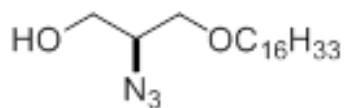
**Fig. 1**



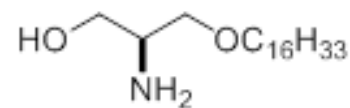
**56-2**



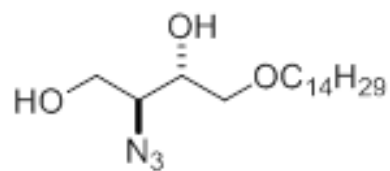
**56-3**



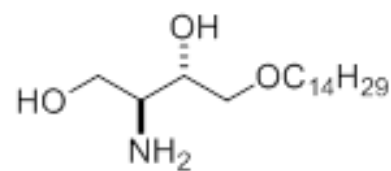
**56-4**



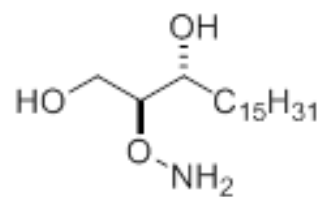
**56-5**



**77-5**



**77-6**



**67-622**

Fig. 2

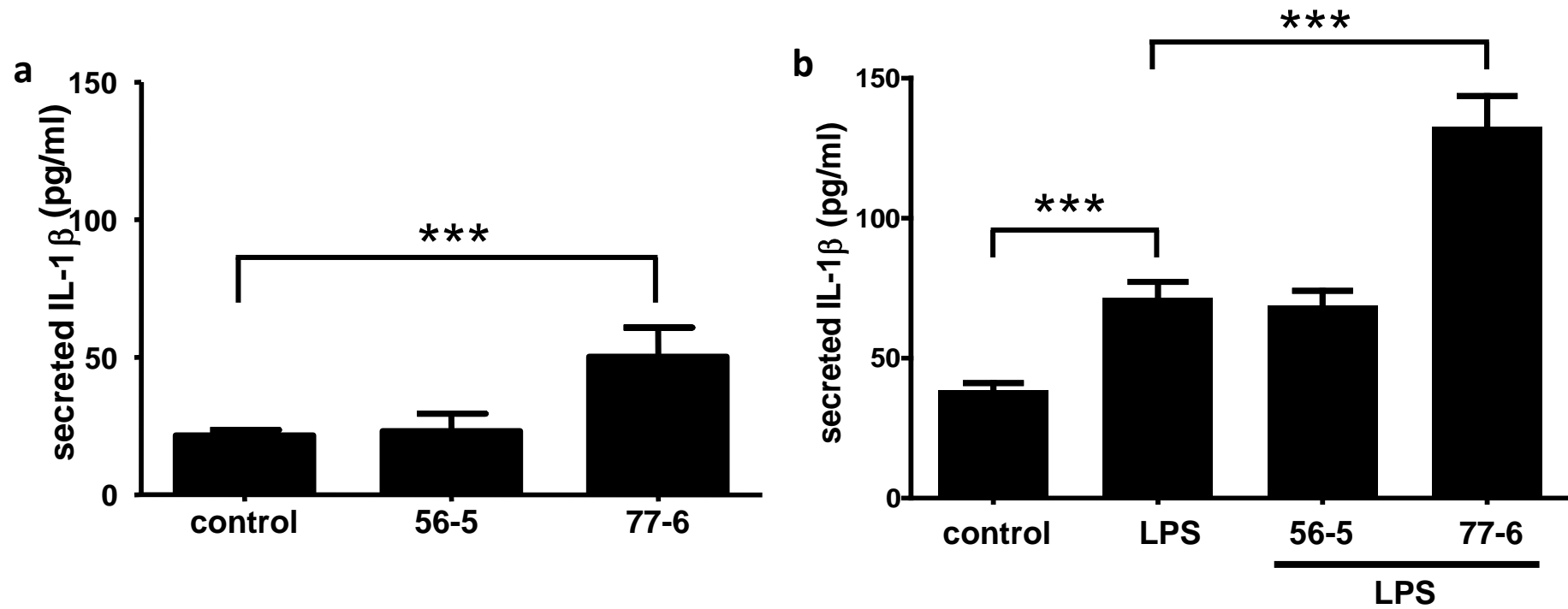


Fig. 3

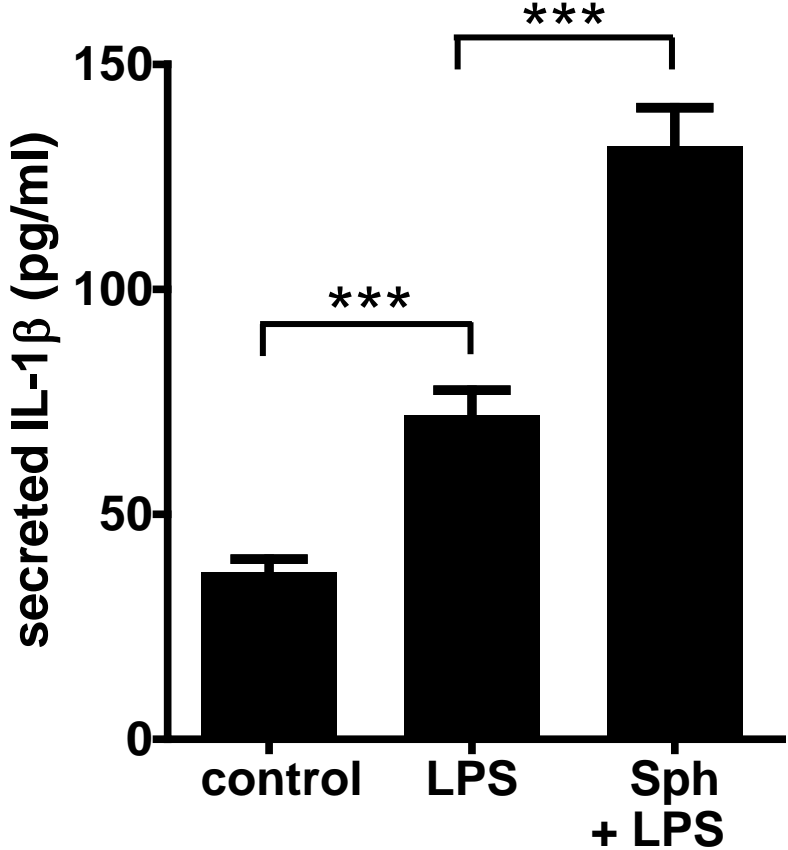


Fig. 4

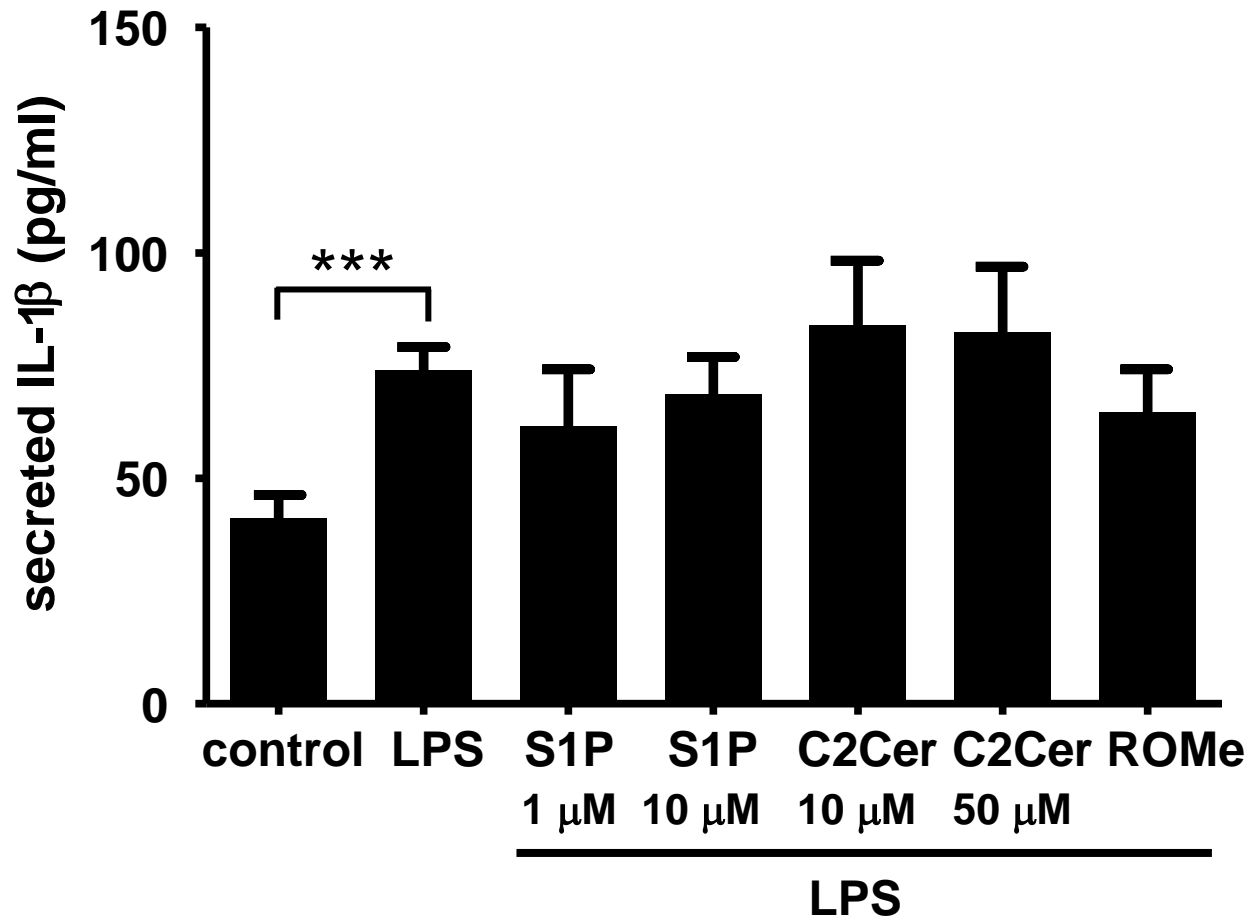


Fig. 5

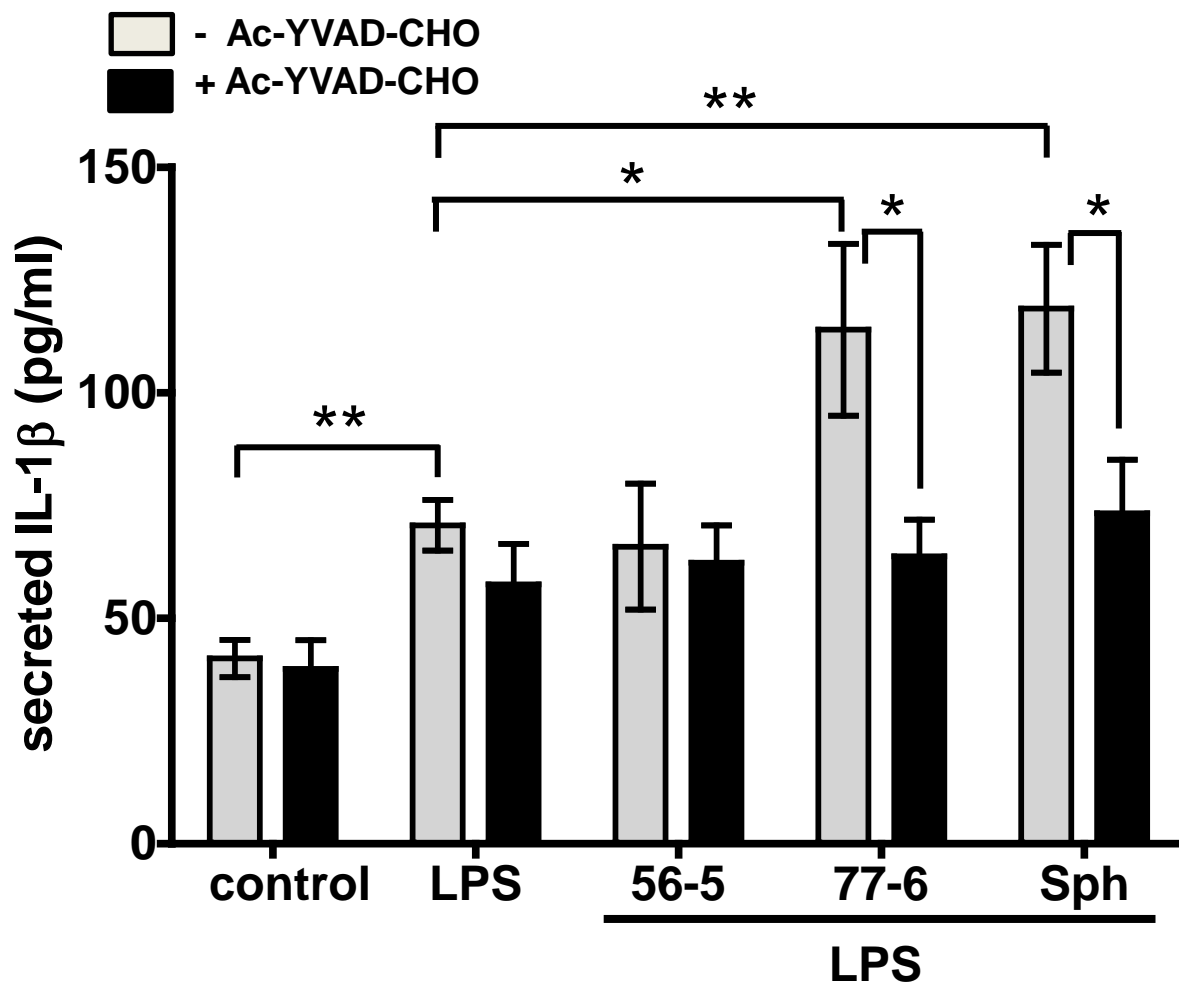


Fig. 6

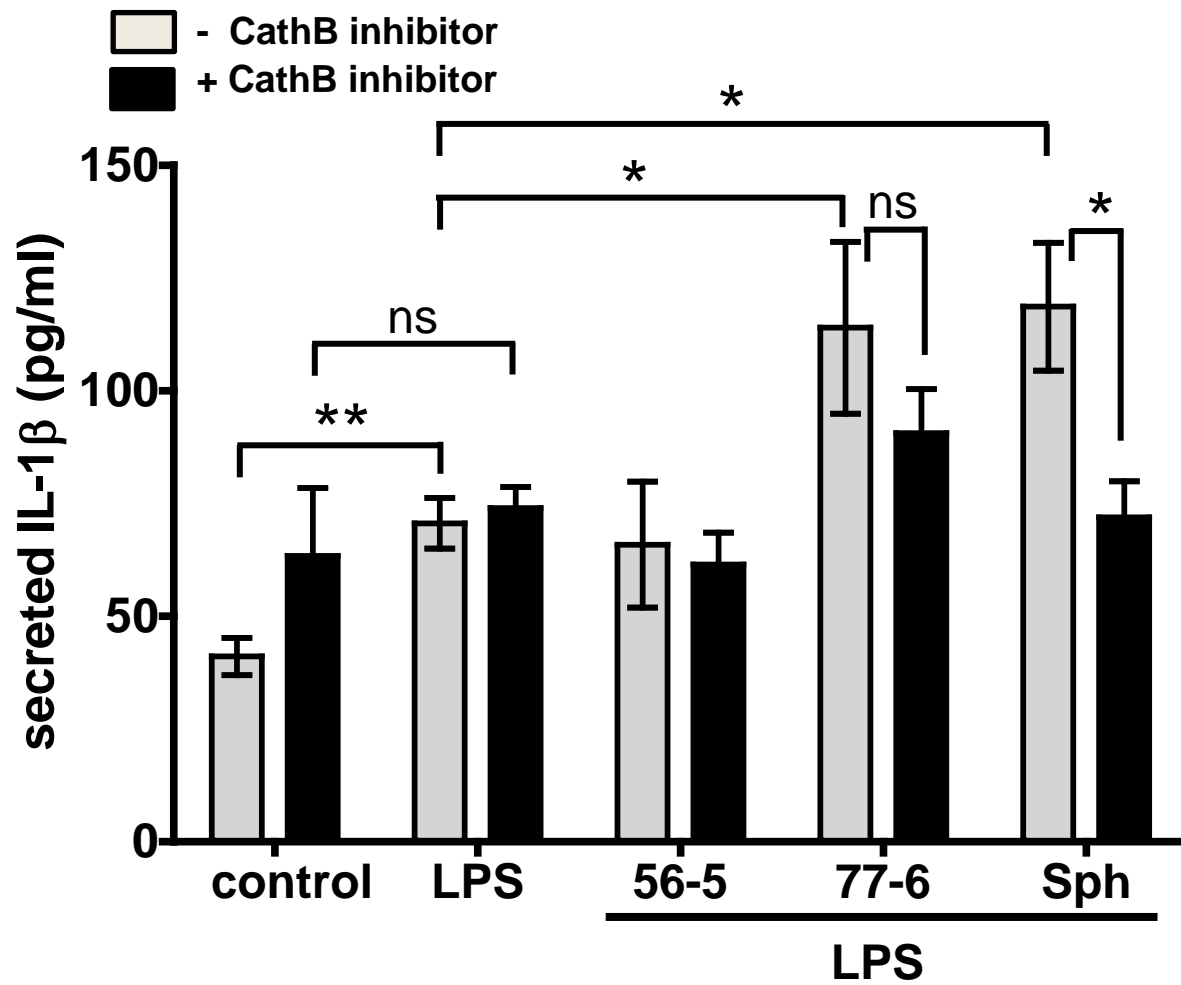


Fig. 7

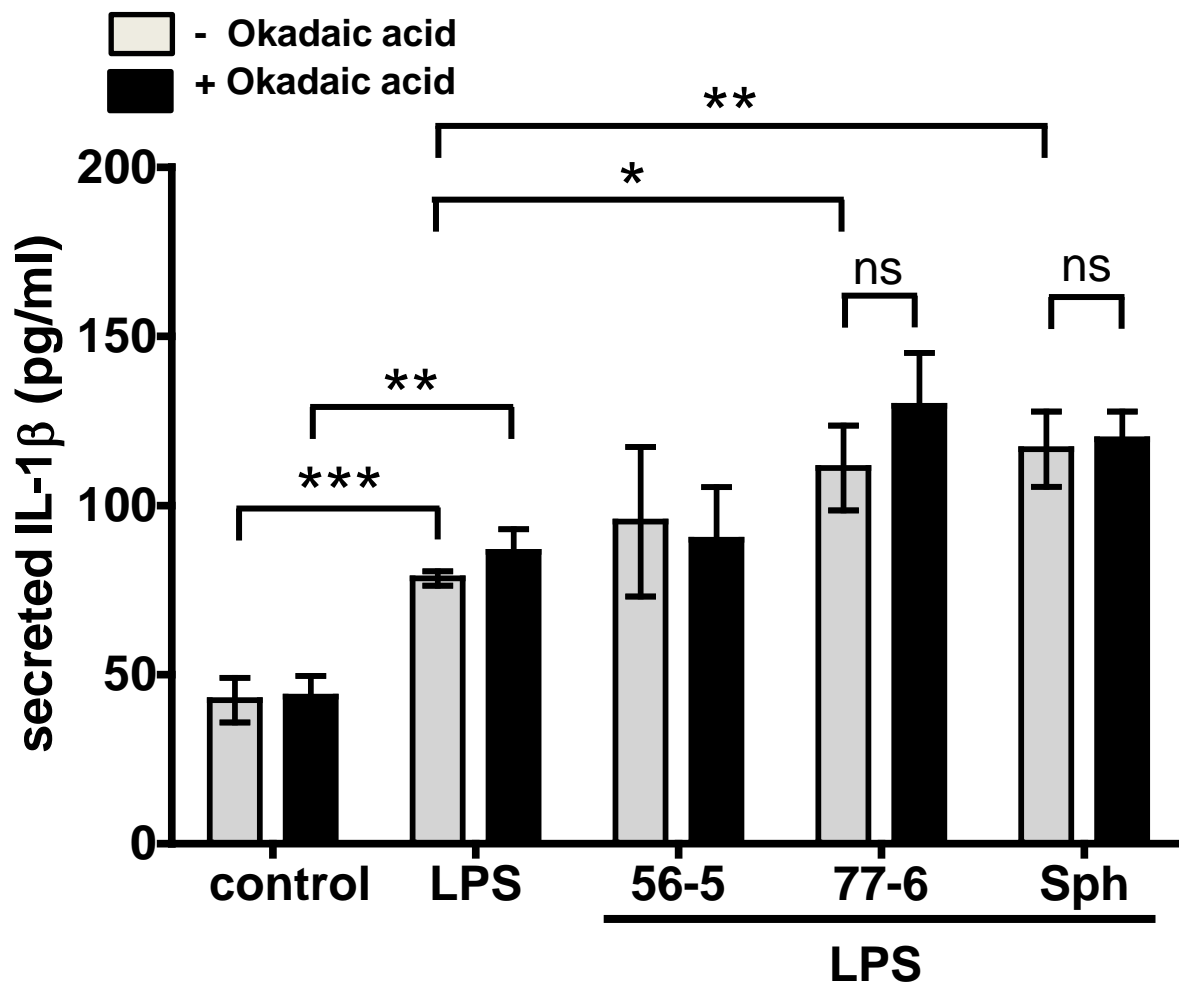


Fig. 8

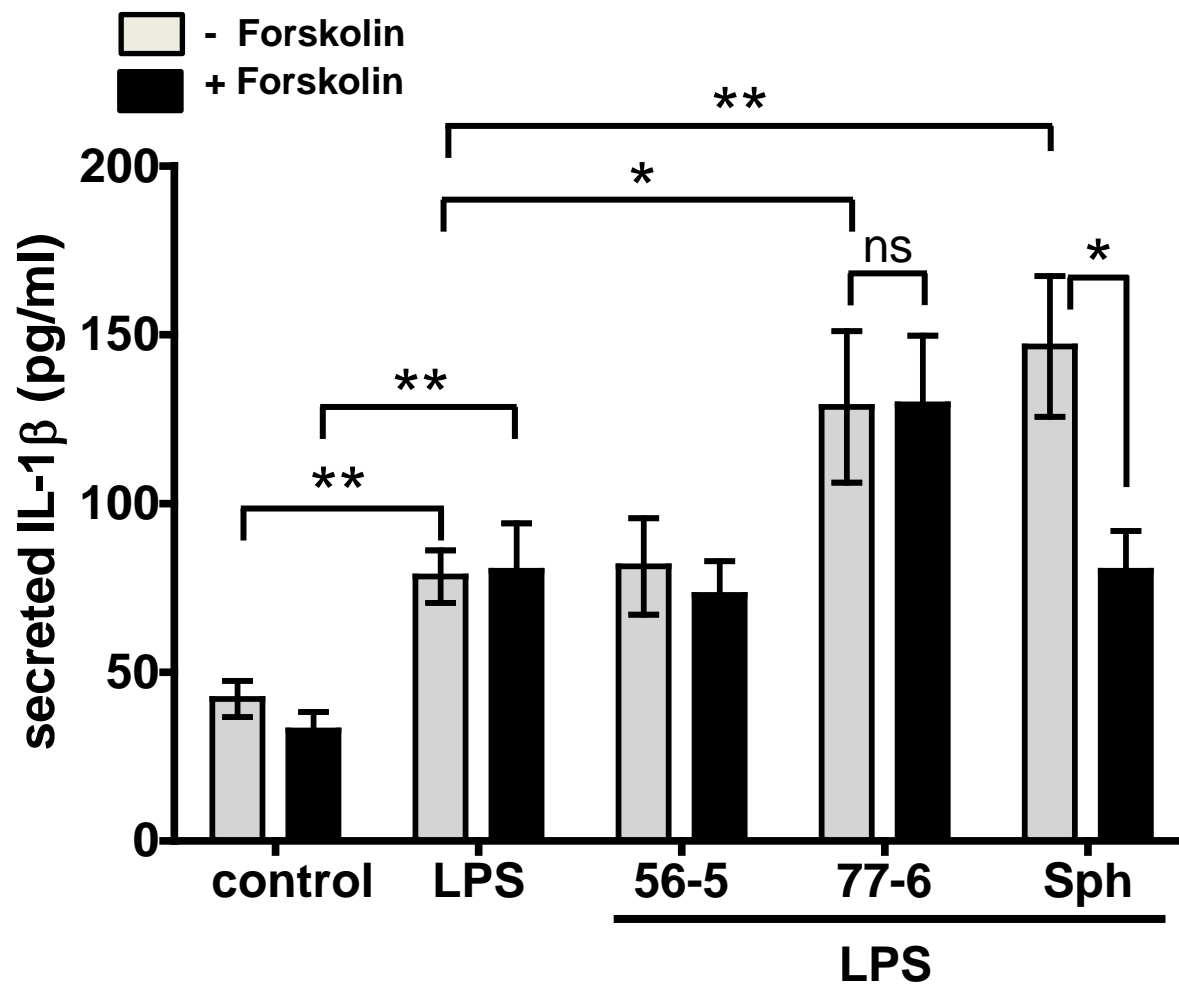


Fig. 9A

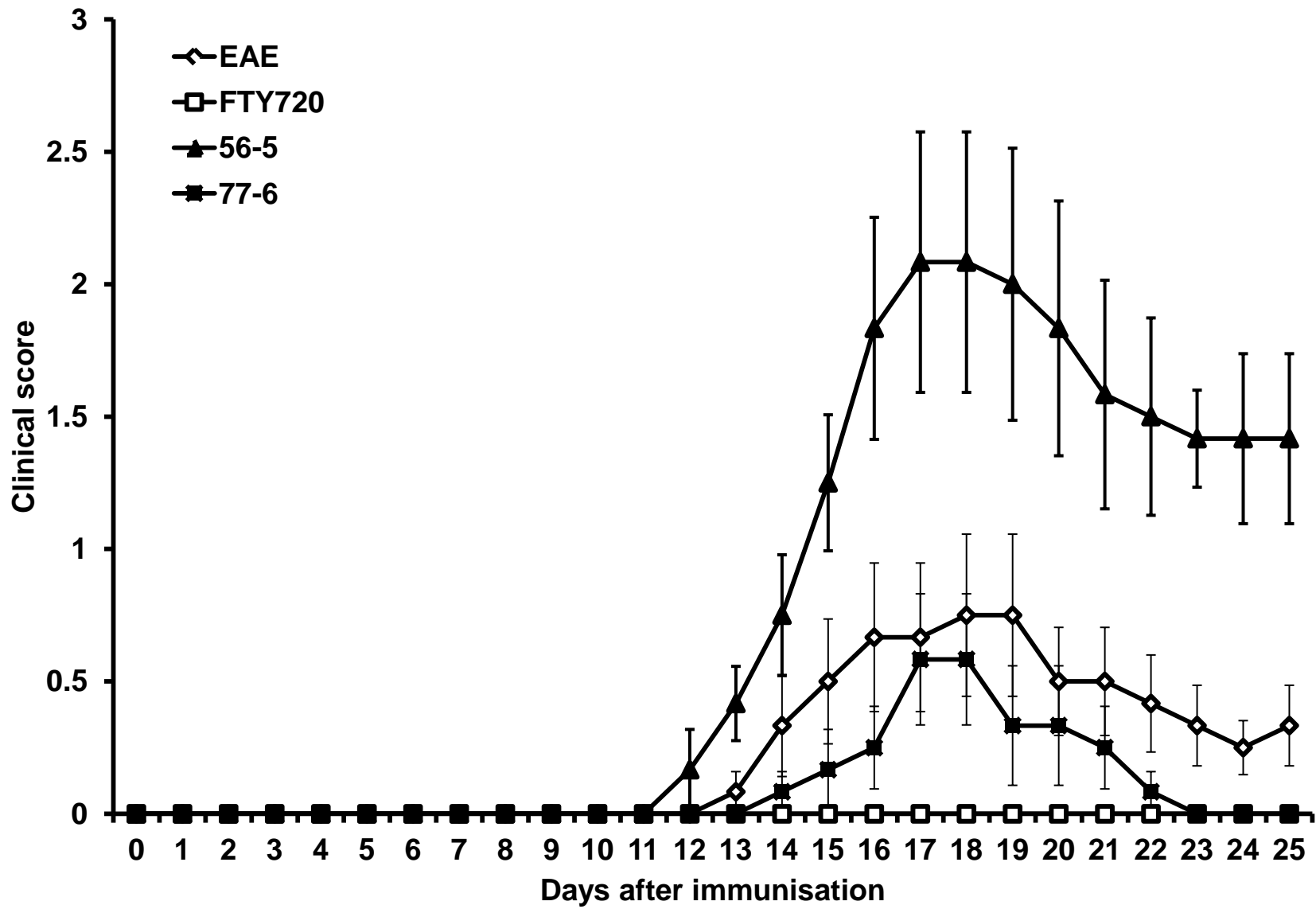


Fig. 9B

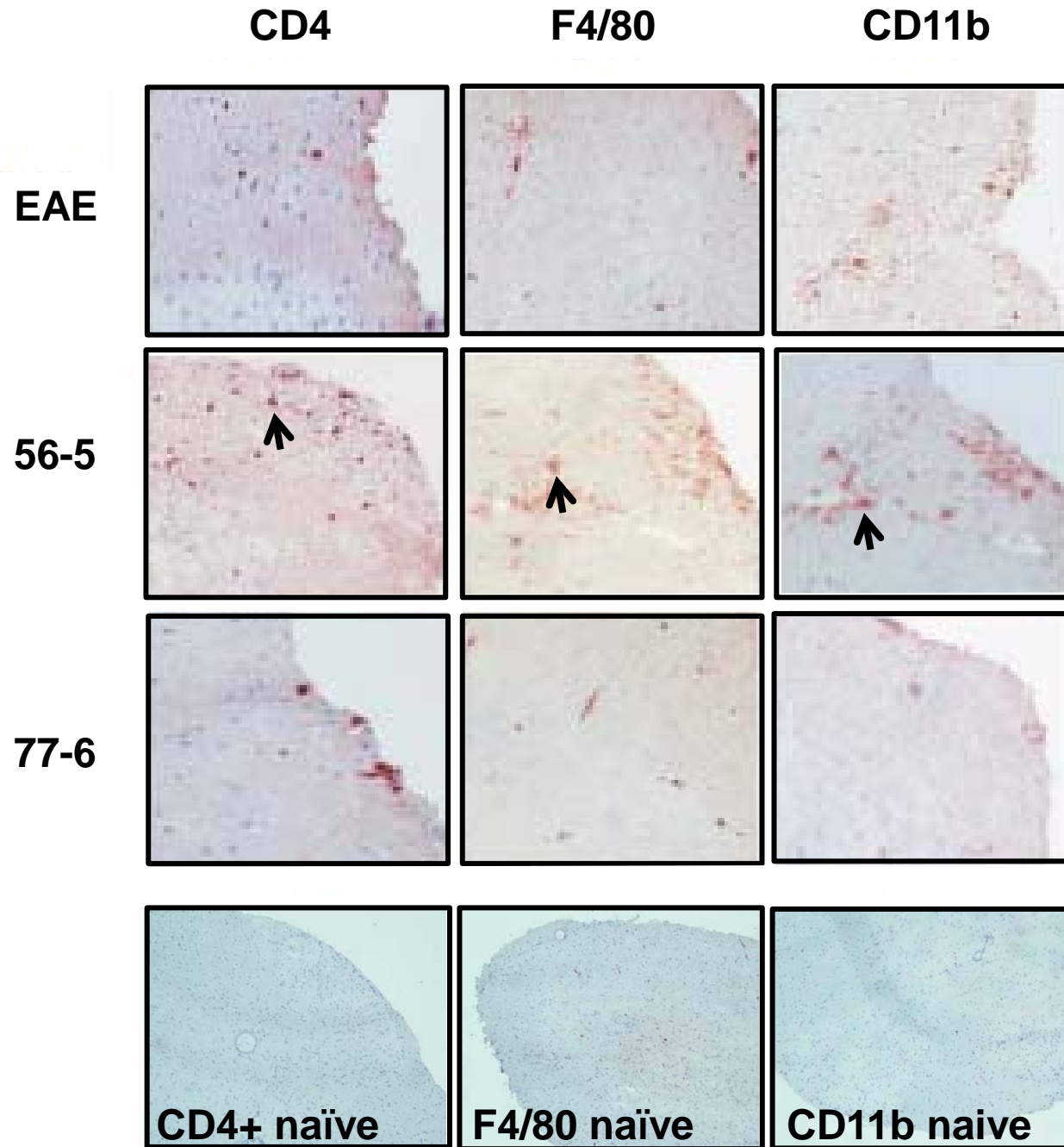


Fig. 10

